Proceedings of the 3rd International Conference on the Frontiers of Plasma Physics and Technology (PC/5099)

LASER PLASMA-INITIATED IGNITION OF ENGINES

J. TAUER[1], H. KOFLER[1], K. ISKRA[2], G. TARTAR[3] and E. WINTNER[1]

[1]Institut für Photonik, Technische Universität Wien, Gusshausstrasse 25-29, A-1040 Wien, Austria
[2]Institut für Experimentalphysik, Technische Universität Graz, Petersgasse 16, A-8010 Graz, Austria
[3]Institut für Verfahrenstechnik, Technische Universität Wien, Getreidemarkt 6, A-1060 Wien, Austria

Abstract

Laser ignition is considered to be one of the most promising future ignition concepts for internal combustion engines. It combines the legally required reduction of pollutant emissions and higher engine efficiencies. The igniting plasma is generated by a focussed pulsed laser beam. Having pulse durations of a few nanoseconds, the pulse energy E_p for reliable ignition amounts to the order of 10 mJ. The lack of adequate compact high-power laser systems on the market with the mentioned specifications led to the development of such a solid-state laser. A fiber-coupled, longitudinally diode-pumped, passively Q-switched solid-state laser was realized. Nd:YAG was chosen as laser active medium emitting at λ_{em} = 1064 nm, and Cr:YAG as passive saturable absorber. A 300 W quasi-cw laser diode as pump source provided pump pulses with energy up to E_{pump}=150 mJ. Experimental studies were carried out to find the optimum component specifications like reflectivity of the output coupler R, initial transmission T_0 of the absorber or optimum in-coupling optics. Single pulse energies of more than 10 mJ at pulse durations of 1.5 ns were yielded. Further on, the in-coupling optics was analyzed in detail in order to draw conclusions with respect to optimum output power. The maximum pulse energy E_p was achieved at R = 60% and $T_0 \approx 60\%$.

1. Introduction

An essential fraction of the surge-current production is based on combined heat and power plants where the mechanical energy of internal combustion engines is employed to power electric generators, and the exhaust gas is used for the exploitation of thermal energy. Consequently, the efficiency of such power plants and hence of the engines must be as high as possible while the pollutant emissions should be kept low. Such requirements cannot be realized satisfactorily any more when using conventional engine ignition techniques. Spark plugs reach their limits at the necessary high ignition pressures demanding for excessively high voltages. However, there are several alternative concepts like plasma ignition, high-frequency ignition, Diesel micro-pilot ignition and laser ignition which might contribute to an improvement of the overall efficiency. To our knowledge, laser ignition represents the most promising future ignition concept out of a number of reasons [1-4]. The main advantages of laser ignition, among many others, are performance enhancing high effective mean pressures in the combustion chamber as well as the feasibility of very lean mixtures lowering the flame temperature and consequently the NO_X emissions.

In general, the mechanism of laser ignition is based on non-resonant gas breakdown [7] of the tightly focused pulsed (ns) laser beam. Initial electrons absorb photons to gain energy via the inverse bremsstrahlung process. These energetic electrons can ionize gas molecules leading to the breakdown in the focal region via the electron cascade growth. It is important to note that this process requires initial seed electrons [8]. These electrons might be produced from thermally heated or linearly ionized impurities like soot or dust in the gas mixture. The plasma formed by the mentioned mechanism can ignite the combustible mixture. Plasma diagnostics revealing shock waves, ignition kernels and flame propagation was observed by high-speed Schlieren photography [5]. The different phases of laser ignition can be defined in chronological order [9]:

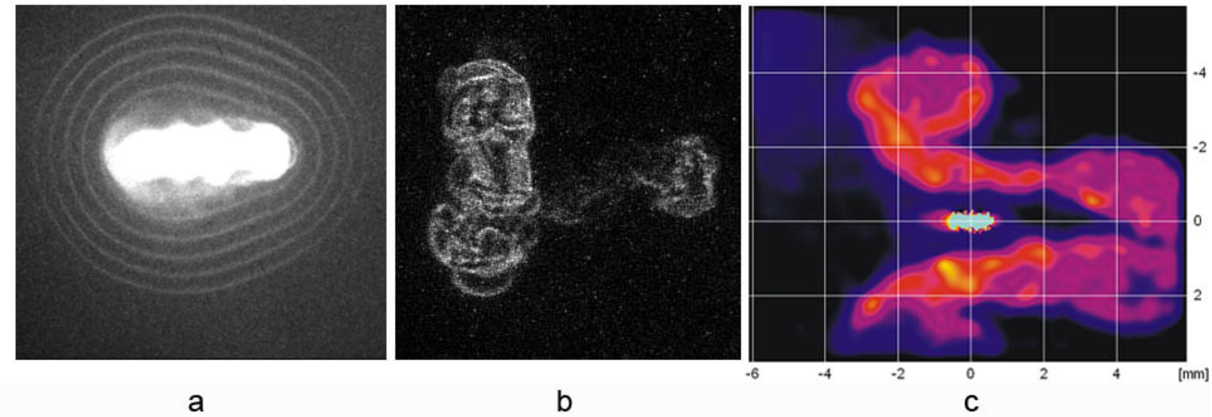

Figure 1: (a) Multi-exposure Schlieren image of shockwave emission around a plasma spark in air at 10 bar in 500-ns steps after ignition. (b) Schlieren image of a stoichiometric methane-air mixture at 10 bar, 500 µs after ignition. (c) Planar Laser-Induced-Fluorescence (PLIF) image of OH-radicals; in all cases, the laser beam enters from the right hand side. [5, 6]

i. Electric breakdown and energy transfer from laser to plasma
ii. Shock-wave generation and propagation
iii. Gasdynamic effects
iv. Chemical induction of branching chain reactions of radicals leading to ignition
v. Turbulent flame initiation

In order to illustrate plasma formation and the onset of combustion, the combined Figure 1 is depicted. The left image (a) threrein shows a multi-exposure image enabling the observation of a shockwave in 500-ns steps. The temporal expansion of the flame kernel is also illustrated using Schieren photography (b) and PLIF imaging (c). The laser pulse entering from the right had an energy $E_p \approx 140$ mJ, the initial pressure of the mixture amounted $p_{in} = 4.3$ bar and the relative air/fuel ratio $\lambda = 1.3$ [6].

Non-resonant breakdown in gases requires intensities of several 10^{11} W/cm² in the focal region [1, 2, 10-13] to be provided by a focused laser pulse with minimum energy $E_p = 0.1$ mJ and pulse durations $\tau_p \leq 10$ ns. For pulses down to several ps the breakdown threshold increases according $\tau_p^{-1/2}$ [8]. Experiments revealing the minimum pulse energies MPE for ignition of different fuel-air mixtures (methane-air, hydrogen-air, methane-hydrogen-air) under engine-like conditions have been reported in former work, partly by our group [1, 2, 10, 14-17]. Furthermore, laser ignition for biogas applications has also been studied successfully [18]. While a plasma can be formed by pulse energies of only a few 100 µJ @ 8ns, the development of a flame kernel requires the more energy in order to ignite the mixture the higher λ and the lower the temperature T is [19]. This circumstance is clearly illustrated in Figure 2. Moreover, for stoichiometric mixtures MPE is independent of T, as it can be seen in the figure.

The higher p_{in} and λ are, the higher is the engine efficiency and the lower are the NO_X emissions, $\lambda \geq 2$ is desirable. In order to ensure reliable ignition for various operation conditions of the gas engine, a ns-laser pulse with $E_p = 5 - 10$ mJ is necessary. Furthermore, we could prove that shorter ns-pulses (≈ 1 ns) are more effective than long ns-pulses (> 10 ns) as the transmission of a plasma decreases with τ_p down to several 100 ps.

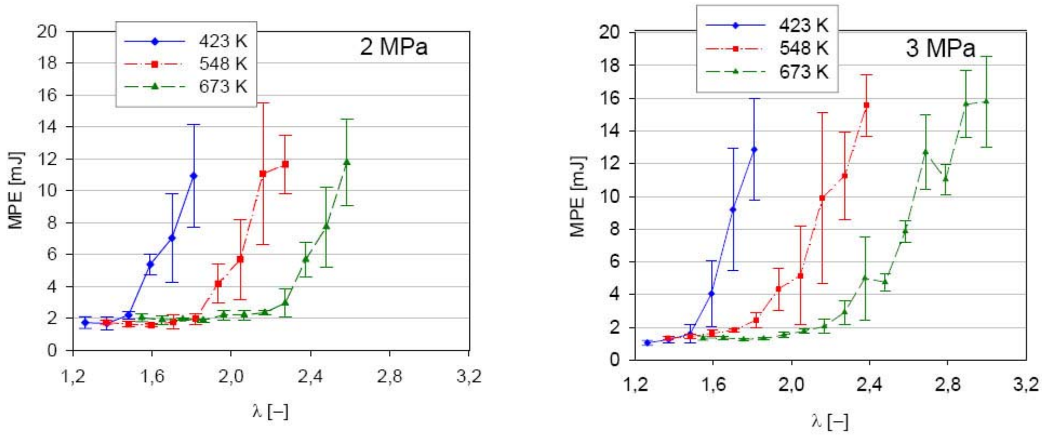

Figure 2: The minimum pulse energy (MPE) versus the relative air/fuel ratio (λ) for different temperatures (T) and initial pressures (p_{in}) of 20 bar (left) and 30 bar (right). The measurements were taken in a constant volume high-pressure vessel [19].

The concept of an optical ignition system emerged in the late 1960ies and has been successively studied by several groups [8, 9, 12, 20, 21]. The coupling of laser radiation into the combustion chamber can be realized by various approaches [21], two of them are:

- A separate ignition laser is mounted on every cylinder head being supplied by an external pump source (laser diode), termed laser spark plug.
- Laser unit and engine are separated and the ignition pulses are transported via optical fibers to the cylinders.

The conceptual ideas and experiments dealing with the development of a compact ignition laser can be found in our recent publication [22]. Such a laser system must be small in size and has to be manufactured in a robust form in order to withstand the adverse influences on the cylinder head. The regime of short ns-pulses can be well covered by passively Q-switched lasers which are, due to their nature, robust, simple in design and cheap. The pump pulse generating the inversion in the laser active medium can be propagated through a conventional optical step-index fiber from an external laser diode to the solid-state laser.

The transportation of ignition pulses via optical fibers implicates some plain advantages, but as a matter of fact, the restrictive factor is the damage threshold of the fiber material. Such pulses may induce intensities in a small core far beyond 1.5×10^9 W/cm² which is the breakdown threshold of fused silica for ns-laser pulses [23, 24]. An enlargement of the solid fiber core area, where the beam is guided, in order to reduce the intensity is not adaptive since for fixed wavelengths higher core diameters imply multi-mode beam profiles. The focusability of the ignition pulse depends strongly on the beam profile, hence disadvantageous multi-mode radiation would enhance the MPE.

However, there exist some concepts for the transportation of ignition laser pulses via hollow-core optical fibers [25-27]. The employment of Photonic Band Gap (PBG) fibers would bring some advantages like single-mode propagation. As reported in a recent paper by our group [28], the highest transmitted single pulse energy of approximately 0.8 mJ is not adequate for laser ignition. The further improvement of hollow fibers has to be successfully achieved before an increase of the delivered pulse energy up to a level sufficient for laser ignition can be realized.

In contrast to the ignition pulse, the pump beam can be guided via conventional optical fibers since the intensity is lower by about six orders of magnitude. In addition, the pump beam generated from diode bars generally is not of single mode nature and therefore only multi-mode fibers are appropriate.

A further cornerstone of laser ignition is the window representing the gateway between the hot combustion chamber and the laser oscillator. Previous investigations on the window include combustion-sided deposits and their formation as well as laser-induced deposit formation. Even a few deposits on the window lead to substantial absorption of laser radiation. Deposits on the combustion window are not well defined substances ranging from nutty, carbonaceous matters to small inorganic particles [29].

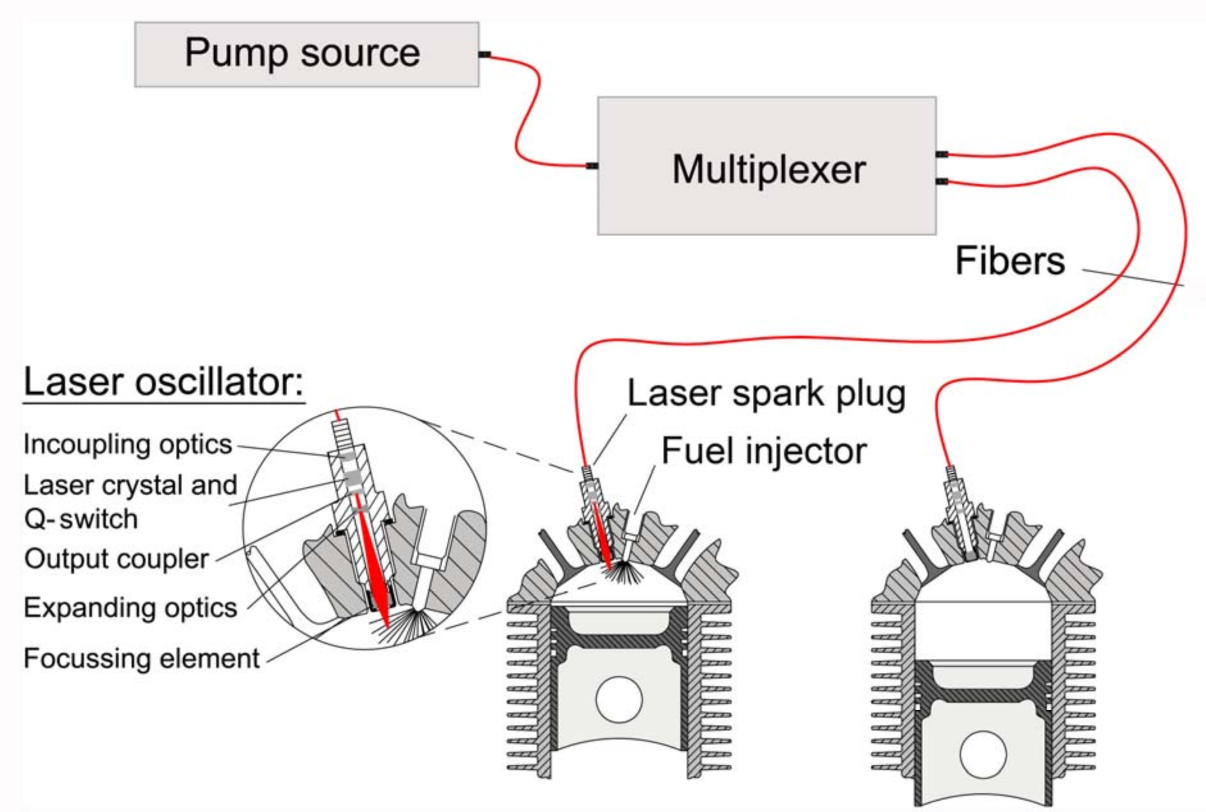

Figure 3: Schematic illustration of the pursued laser ignition concept. Each laser on a cylinder head is supplied by the external pump source via a separate optical fiber. The multiplexer distributes the pump radiation from the common pump source to each fiber.

The ignition laser system must fulfill the afore mentioned requirements in order to ensure reliable operation under engine-like conditions. Unfortunately, such small ns-pulsed laser systems are commercially not available. Moreover, customary laser systems fulfilling the needs of laser ignition are large in size, heavy, expensive and consume several kilowatts of electrical power. Thus the need to develop an ignition laser of our own emerged

An end-pumped fiber-coupled passively Q-switched solid-state laser seems to be the most promising candidate. Such a laser system satisfies the requirements like compactness, robustness, low cost and the pumpability via optical fibers. Figure 3 shows the schematic concept of laser ignition applying a laser spark plug with an external pump source. Besides this advantageous concept, other research groups favour the idea of a transversally-pumped solid-state laser for ignition. To our knowledge, transversally-pumped laser systems are worse in beam quality and pulse duration. Moreover, such side-pumped systems are more complex and expensive than end-pumped ones. The following section introduces the schematic setup of the laser system as well as the experimental setup.

2. Experimental Setup

A suitable laser ignition system covering the requirements like robustness, simple design and compactness is a fiber coupled, end-pumped passively Q-switched solid-state laser. Figure 4 depicts the schematic setup of such a laser unit. Beside the financial aspect the availability of the components is a major point within the selection criteria. Therefore Nd^{3+}:YAG as laser active medium and Cr^{4+}:YAG as passive absorber has been chosen.

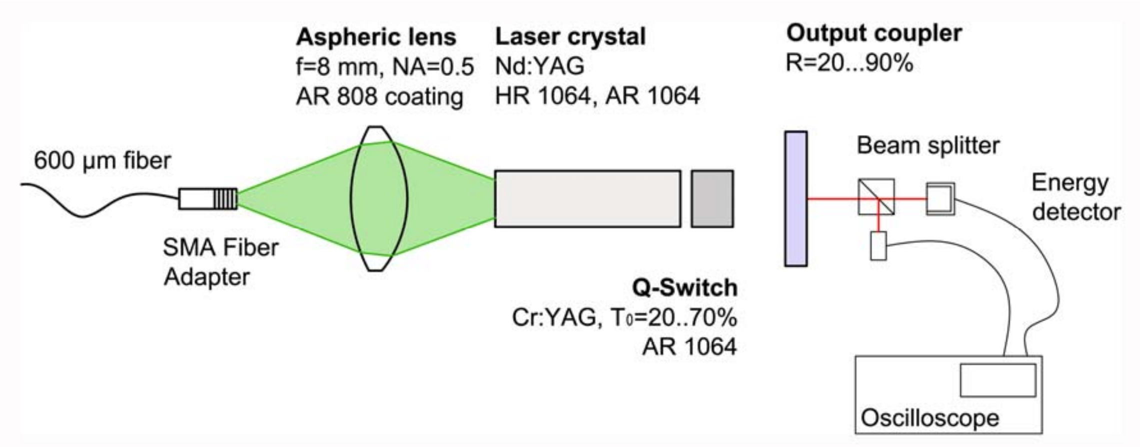

Figure 4: Schematic view of the laser system. The pulse length was measured by a photodiode while for the energy measurement a pyroelectric sensor was used.

The Nd-doping of the laser crystal was around 1.0 at. % and the fluorescence lifetime of the upper laser level $^4F_{3/2}$ amounts to $\tau_{fl} \approx 255$ µs. The absorption line of Nd^{3+}:YAG is centered around $\lambda_{diode} = 808$ nm being suitable for a GaAs high power laser diode as pump source. Pump pulses up to a power $P_{pump} = 300$ W @ 500 µs can be generated by this laser diode. Since the laser diode shows a temperature gradient of 0.3 nm/K, temperature stabilization was necessary. Furthermore, as shown in Figure 5, temperature stabilization enables the exact adjustment of the diode emission line and the crystal absorption wavelength with the aim of highest conversion efficiency. A step-index fiber for transportation of the pump pulse with a core diameter of 600 µm and a numerical aperture NA = 0.22 were employed.

Different aspheric collimating lenses with effective focal lengths $l_{f,eff} = 1.5 - 18$ mm were tested, however, the lens with $l_{f,eff} = 8$ mm and NA = 0.5 turned out to be the most suitable for in-coupling the pump beam into the laser crystal.

The in-coupling mirror of the resonator was directly coated onto the crystal in order to reduce the length of the system and, as a result, the pulse duration. Moreover, the end face of the crystal was coated with an anti-reflection (AR) layer for the 808 nm pump beam reducing the reflection losses. The output-coupler was separated from the crystals since the adjustment of the mirror allows flexibility in pulse energy and beam profile.

Passive absorbers with initial transmissions $T_0 = 25\% - 70\%$ and output-couplers with reflectivities $R = 25\% - 90\%$ cover the field of laser operation. All passive absorber crystals were coated with an AR layer for the laser wavelength $\lambda_{em} = 1064$ nm. In order to achieve highest output power the in-coupling optics were always adapted with respect to the resonator conditions (length, reflectivity, initial transmission). The results are summarized in the next section.

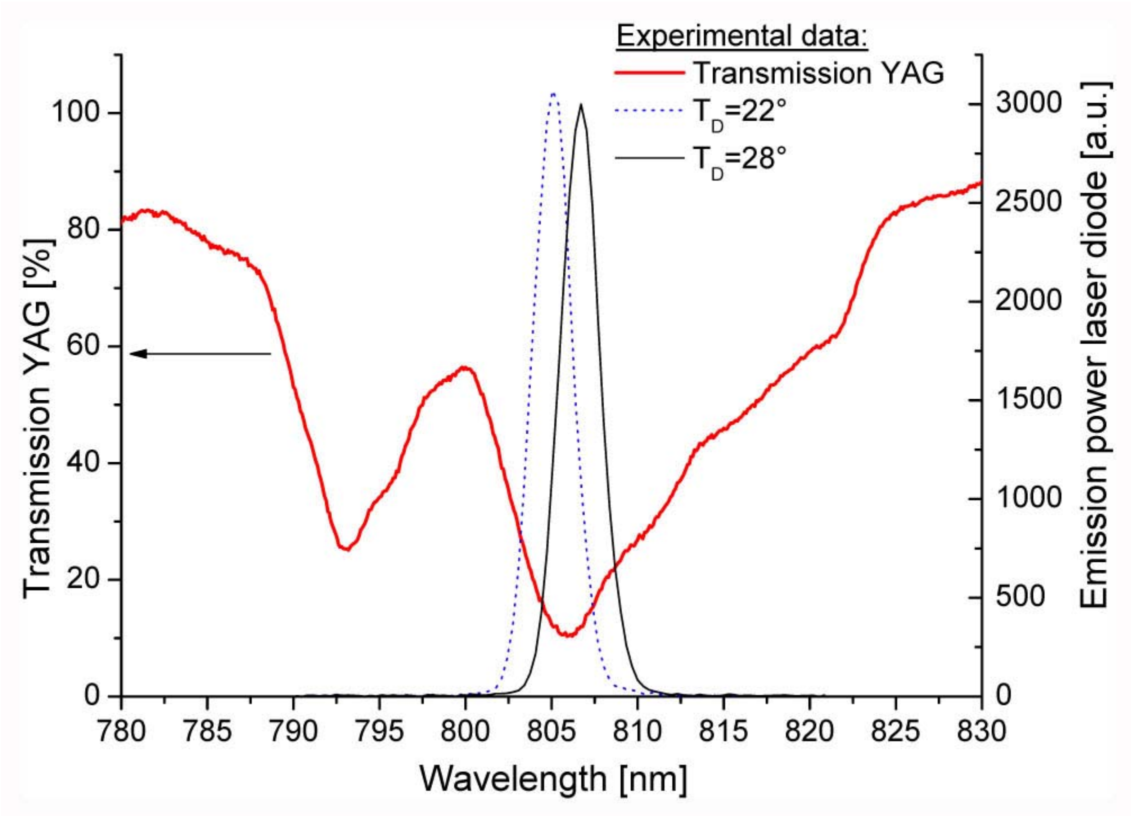

Figure 5: Emission and absorption spectrum of the laser diode and the laser crystal, respectively. At a emission wavelength λ_{diode} = 805.7 nm, corresponding to a diode temperature (T_{diode}) of approximately 26°C, the maximum absorption (minimum transmission) was noted.

3. Results

The main parameters strongly influencing the maximum output power are the pump duration τ_{pump}, T_0 and R. At a pump power P_{pump} = 70 W, τ_{pump} = 300 µs, R = 50% and T_0 = 40% the maximum pulse energies of approximately 2.1 mJ were yielded. This result corresponds to an optic-to-optic efficiency η_{optic} = 7.1%. The length of the resonator was about 15 mm while the length of the Nd-doped laser rod having ø = 2 mm thickness was 5 mm. Pulse durations $\tau_p \approx$ 1.0 ns were achieved leading to a peak power $P_{p,peak}$ > 2 MW.

An additional parameter influencing E_P is the crystal doping being typically between 0.8 – 1.4 at.%. However, some manufacturers offer 2.5 at.%-doped Nd:YAG crystals which result in a higher cross-section and, therefore in higher absorption efficiency, but the fluorescence life-ime τ_{fl} decreases dramatically. For our purposes, a compromise between the absorption efficiency and the storage ability of the upper laser level had to be found. It turned out that Nd-doping around 1.4 at.% led to the maximum output power.

An increase of P_{pump} = 300 W and τ_{pump} = 300 µs lead to $E_p \approx$ 6 mJ at $\tau_p \approx$ 1.0 ns using the in-coupling lens shown in Figure 4, but with an effective focal length $l_{f,eff}$ = 4.6 mm. We found out, that E_p is very sensitive to τ_{pump} due to the thermal load of the laser crystal. Figure 6 depicts the experimental data of E_p versus τ_{pump}.

However, above $\tau_{pump} \approx$ 200 µs E_p remains constant at a value of roughly 6 mJ. Furthermore, the timing jitter being the fluctuation of the temporal position of the pulse increases dramatically for large τ_{pump} and the laser system becomes unstable. The afore mentioned in-coupling optics plays also a major role concerning the laser output. Employing the 11 and 15.3 mm aspheric lenses, the yielded pulse energy was much lower than when using the 4.6 and 8 mm lens. The focal spot of the 11 and 15.3 mm lenses were larger than the end-face of the crystal and, therefore, a certain amount of pump energy could not be employed to create inversion.

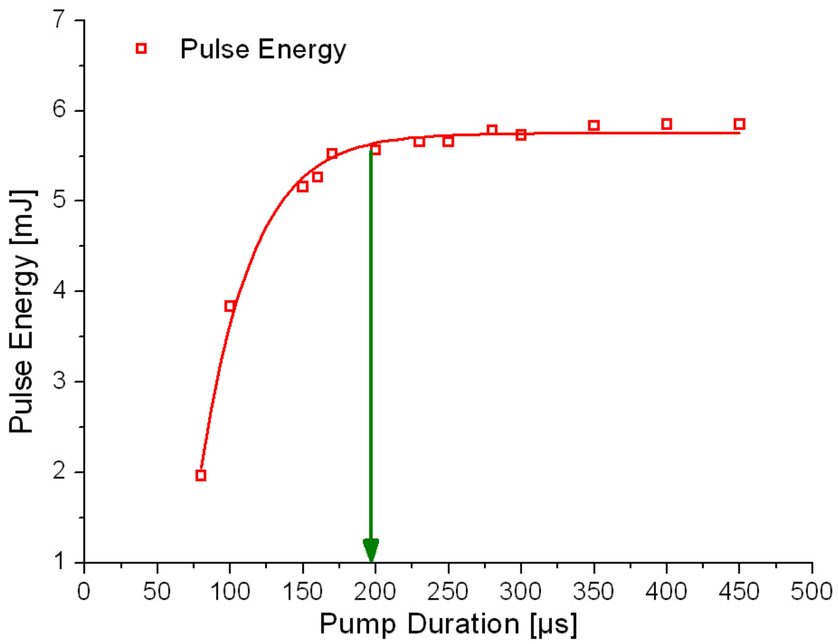

Figure 6: The pulse energy (E_p) versus the pump duration (τ_{pump}). At a certain $\tau_{pump} \approx 200$ µs E_p does not rise any more.

Using a ø = 5 mm thick and l = 10 mm long laser rod, the pump beam absorption efficiency could be increased and, as a consequence, E_p. On the one hand, a lens with a higher effective focal length (and consequently larger focal spots) can be applied and, on the other hand, longer crystals can absorb the pump beam more efficiently according to Beer's law.

Employing output couplers with R = 40 and 60%, and absorbers with T_0 = 10 – 60%, as shown in Figure 7, led to E_p ranging from 7 to 10 mJ. These output values correspond to η_{optic} > 11%. In this case again τ_{pump} = 300 µs, but in contrast to the 2 mm-thick crystal, an increase of E_p in the range of τ_{pump} = 200 – 300 µs was observed. This experimental fact might be due to the larger inversion volume and the reduced thermal load per volume. The used in-coupling lens had an effective focal length of $l_{f,eff}$ = 8 mm and a NA = 0.50 enabling good illumination of the laser rod. τ_p is in the order of 1.5 ns corresponding to a peak power $P_{p,peak}$ > 6 MW representing a respectable value for such a compact solid-state laser. The slightly longer pulse duration τ_p =1.5 ns in comparison to the above mentioned pulses with energies of 2 and 6 mJ is due to a higher T_0 = 60% of the saturable absorber.

Recapitulating, this improvement in performance is due to the thicker laser crystal, on the one hand, and due to a more efficient in-coupling process, on the other hand. A further interesting aspect is the intensity profile of the outgoing beam. While the intensity distribution for pulse with E_p = 2 mJ is quasi-Gaussian (Figure 8a), the profile for pulses with energies E_p = 6 and 10 mJ is somewhat different. In addition to the fundamental Gaussian mode higher TEM_{lm} modes can oscillate [30]. In our case, we observed TEM_{10} for E_p = 6 mJ (Figure 8b) and TEM_{20} (Figure 8c) for E_p = 10 mJ.

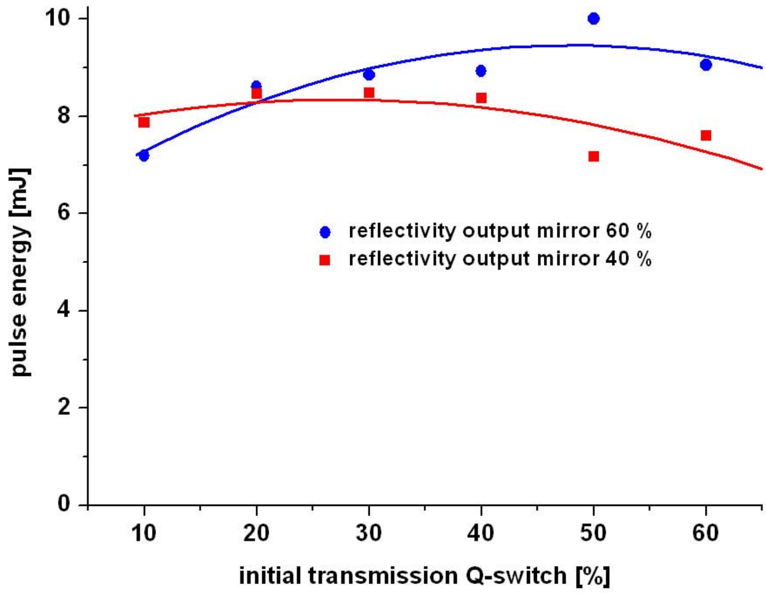

Figure 7: The pulse energy (E_p) as a function of the initial transmission (T_0) and two different reflectivities (R) of the output coupler.

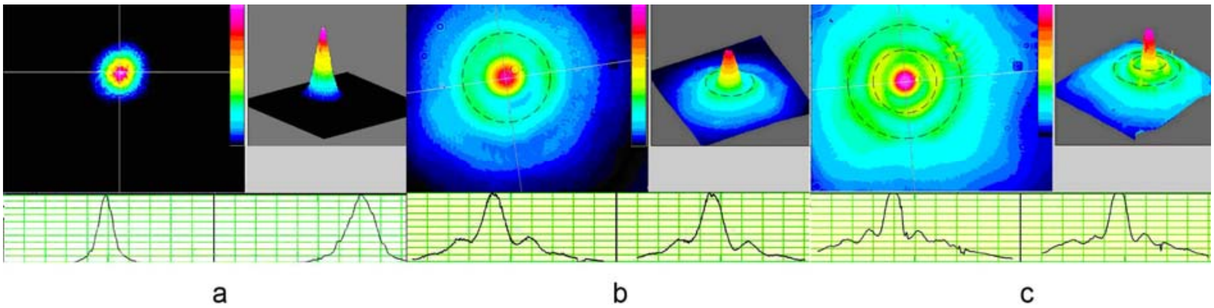

Figure 8: Observed transversal modes of the outgoing laser beam. For pulse energies E_p in the order of 2 mJ (a) the distinctive Gaussion mode can be seen. For higher energies (in (b), E_p = 6 mJ, in (c), E_p = 10 mJ)) also higher modes are present.

The presence of additional higher modes is due to the thicker volume where inversion is created. Since the pump beam diameter is enlarged also the laser active volume increased leading to higher pulse energy.

4. Discussion

Although passively Q-switched solid-state lasers using Nd:YAG as active medium are well-known and field tested with respect to many applications [31-35], we spent various investigations towards an optimization of E_P at pulse length in order the of 1 ns. The special requirements of laser ignition with respect to pulse energy could be satisfactorily fulfilled by our system. Taking the maximum pulse energy of 10 mJ at a pulse duration of approximately 1.5 ns into account, the creation of a plasma in air under atmospheric condition is possible. Therefore, also fuel/air mixtures can be ignited with this laser unit since the plasma breakdown thresholds of combustible gases are in the same order of magnitude as air. Furthermore and most importantly, the output power of 10 mJ @ 1.5 ns is sufficient to also feed the flame kernel of the combustion in case of very lean mixtures.

This improvement of pulse energy is mostly a consequence of optimized in-coupling optics and thicker laser crystals. To our knowledge, these output parameters E_p = 10 ns @ τ_p = 1.5 ns corresponding to an optic-to-optic efficiency η_{optic} > 11% are unique due to the fact that no low-repetitive, self-Q-switched, high-peak power and compact lasers have been developed and published up till now. In [32] a compact monolithic passively Q-switched Cr,Nd:GSGG microlaser with a single-pulse energy of several 100 µJ at τ_p = 1.5 ns was reported. Further experimental studies on compact, longitudinal diode-pumped Nd:YAG laser employing V^{3+}:YAG as saturable absorber have been discussed in [34]. The maximum observed pulse energy therein was E_p = 131 µJ at τ_p = 6 ns and an η_{optic} = 2.7%. Another small Nd-doped laser has been published in [35] using a 600 W quasi-cw diode. The achieved output parameters of the 11 mm long resonator were pulse durations of about τ_p = 4 ns and pulse energies E_p = 4.5 mJ. An interesting pump arrangement, where the laser rod was pumped at both end-faces leading to better absorption efficiency can be found in [33]. Nevertheless, such a laser setup is not useful for our purposes since the ignition laser should be assembled into a small, rod-like housing.

5. Conclusion and outlook

This paper reviews the milestones of laser ignition in short, being based on laser-induced plasma formation, and the corresponding ignition parameters. These facts give information about the relevant laser specifications. The basic requirements which are pulse energies around 10 mJ at pulse durations of about 1 ns were realized. For a realistic application to combustion engines, the laser system should be assembled in small housing with dimensions of a conventional spark plug. Moreover, the laser system has to withstand the detrimental influences of the engine inherent vibrations as well as thermal and mechanical stresses. One of the promising ways to meet these requirements will be a monolithic laser design.

Acknowledgements

G. Herdin and J. Klausner deserve special thanks for their helpful discussions. Financing by the company GE Jenbacher GmbH & Co OHG, Austria, and by the Austrian Industrial Research Promotion Fund under Grant FFF 803050 is greatfully acknowledged. Last but not least, our appreciation is expressed to G. Reider for his helpful laser related discussions.

References

[1] H. KOPECEK, et al., *"Laser ignition of methane-air mixtures at high pressures and diagnostics"*, Journal of Engineering for Gas Turbines and Power, Vol. 127(1), pp.213-219, (2004).

[2] H. KOPECEK, et al., *"Laser-induced ignition of methane-air mixtures at pressures up to 4MPa"*, Laser Physics Letters, Vol. 13(11), pp.1-5, (2003).

[3] H. KOPECEK, et al., *"Laser-stimulated Ignition in a Homogeneous Charge Compression Ignition Engine"*, SAE International, (2003).

[4] P. D. RONNEY, *"Laser versus conventional ignition of flames"*, Optical Engineering, Vol. 33(2), pp.510-521, (1994).

[5] M. LACKNER, et al., *"Investigation of the early stages in laser-induced ignition by Schlieren photography and laser-induced fluorescence spectroscopy"*, Optics Express, Vol. 12, pp.4546-4557, (2004).

[6] M. LACKNER, et al. "*Optical Diagnostics of Laser Ignition for Future Advanced Engines*", Proceedings of ASME Fall Technical Conference, (2004).

[7] L. J. RADZIEMSKI, et al., "*Laser-Induced Plasmas and Applications*", Thompson Brian J., 1 ed., New York, Marcel Dekker Inc., pp. 445, ISBN: 0-8247-8078-7, (1989).

[8] T. X. PHUOC, *"Laser-induced spark ignition fundamental and applications"*, Optics and Lasers in Engineering, Vol. 44(5), pp.351-397, (2006).

[9] D. BRADLEY, et al., *"Fundamentals of high-energy spark ignition with lasers"*, Combustion and Flame, Vol. 138(1-2), pp.55-77, (2004).

[10] H. KOPECEK, et al., *"Laser ignition of methane-air mixtures at high pressures"*, Experimental Thermal and Fluid Science, Vol. 27, pp.499-503, (2003).

[11] H. KOPECEK, et al. "*Laser-induced ignition characteristics of methane- and hydrogen-air mixtures at high pressures*", Proceedings of SPIE, Vol. 5506, (2004).

[12] T. X. PHUOC, *"Laser spark ignition: Experimental determination of laser - induced breakdown of combustion gases"*, Optics Communications, Vol. 175(4), pp.419-423, (2000).

[13] M. WEINROTTER, et al., *"Application of laser ignition to hydrogen-air mixtures at high pressures"*, International Journal of Hydrogen Energy, Vol. 30(3), pp.319-326, (2004).

[14] M. WEINROTTER, et al., *"An extensive comparison of laser-induced plasma ignition and conventional spark plug ignition of lean methane-air mixtures under engine-like conditions"*, SAE Technical Paper Series, Vol. 1972, pp.248-256, (2005).

[15] M. WEINROTTER, et al., *"Laser ignition of ultra-lean methane-hydrogen-air and hydrogen-air mixtures under engine-like conditions"*, Experimental Thermal and Fluid Science, Vol. 29(5), pp.569-577, (2005).

[16] J. L. BEDUNEAU, et al., *"Measurements of minimum ignition energy in premixed laminar methane/air flow using laser induced spark"*, Combustion and Flame, Vol. 132, pp.653-665, (2003).

[17] D. H. MCNEIL. "*Minimum Ignition energy for laser spark ignition*", Proceedings of Combustion Insitute, Vol. 30, (2005).

[18] C. FORSICH, et al., *"Characterization of Laser-Induced Ignition of Biogas-Air Mixtures"*, Biomass & Bioenergy, Vol. 27(3), pp.299-312, (2004).

[19] M. WEINROTTER, et al. "*Laser ignition of engines – a realistic option!*" Proceedings of SPIE, Vol. 6053.

[20] J. D. DALE, et al., *"Laser Ignited Internal Combustion Engines - An Experimental Study"*, SAE Technical Paper Series, Vol. 780329, (1978).

[21] M. WEINROTTER, et al., *"Laser ignition of engines"*, Laser Physics, Vol. 15(7), pp.947-953, (2005).
[22] H. KOFLER, et al., *"An Innovative Solid-State Laser for Engine Ignition"*, Laser Physics Letters, Vol. 4(6), pp.322-327, (2007).
[23] B. C. STUART, et al., *"Laser-Inducerd in Dielectrics with Nanosecond to Subpicosecond Pulses"*, Physical Review Letters, Vol. 74(12), pp.2248-2251, (1995).
[24] R. WOOD, *"Laser damage in optical materials at 1.06µm"*, GEC Journal of Science & Technology, Vol. 45(3), pp.109-115, (1979).
[25] Y. MATSUURA, et al. "*Hollow fibers for delivery of high-power lasers*", Proceedings of SPIE, Vol. 4065, (2000).
[26] A. YALIN, et al., *"Use of hollow-core fibers to deliver nanosecond Nd:YAG laser pulses to form sparks in gases"*, Optics Letters, Vol. 30(16), pp.2083-2085, (2005).
[27] A. YALIN, et al. "*Fiber Delivered Systems for Laser Ignition of Natural Gas Engines*", Proceedings of ASME Internal Combustion Engines Division, (2006).
[28] J. TAUER, et al., *"High-throuput of single high-power laser pulses by hollow photonic band gap fibers"*, Laser Physics Letters, Vol. 4(6), pp.444-448, (2007).
[29] H. KOFLER, et al. "*Fenster zur Verbrennungsdiagnostik: Herabsetzung der Verschmutzungsneigung für einen störungsfreien Langzeitbetrieb*", Proceedings of VDI Vol. 1888, (2005).
[30] W. KOECHNER, et al., "*Solid-State Laser, A Graduade Text*", Springer, pp. 409, ISBN: 0-387-95590-9, (2003).
[31] G. HENNIG, et al. "*Laser engraving in gravure industry*", Proceedings of SPIE, Vol. 6157, (2005).
[32] R. L. SCHMITT, *"Monolithic passively Q-switched Cr:Nd:GSGG microlaser"*, Proceedings of SPIE - The International Society for Optical Engineering Volume 5871, 2005, Article number 587105, Pages 1-8.
[33] S. K. SUDHEER, et al., *"Set temperature dependence of fractional thermal loading and effective stimulated emission cross section of a diode double end pumped* TEM_{00} *Nd:YAG laser for micromachining application"*, Laser Physics Letters, Vol. 3(5), pp.244-248, (2006).
[34] J. SULC, et al., *"Nd:YAG/V:YAG microchip laser operating at 1338 nm"*, Laser Physics Letters, Vol. 2(11), pp.519-524, (2005).
[35] W.-Q. WEN, et al., *"Short cavity passive Q-switched Nd:YAG laser end-pumped by QCW-LDA "*, Journal of Optoelectronics Laser, Vol. 13(9), pp.900-903, (2002).